A Light-Weight Interpretable Model for Nuclei Detection and Weakly-Supervised Segmentation

Yixiao Zhang[1(✉)], Adam Kortylewski[2], Qing Liu[3], Seyoun Park[1], Benjamin Green[1], Elizabeth Engle[1], Guillermo Almodovar[1], Ryan Walk[1], Sigfredo Soto-Diaz[1], Janis Taube[1], Alex Szalay[1], and Alan Yuille[1]

[1] Johns Hopkins University, Baltimore, MD 21218, USA
yzhan334@jhu.edu
[2] Max Planck Institute for Informatics, 66123 Saarbrücken, Germany
akortyle@mpi-inf.mpg.de
[3] Adobe Systems, Inc., San Jose, CA 95110, USA

Abstract. The field of computational pathology has witnessed great advancements since deep neural networks have been widely applied. These networks usually require large numbers of annotated data to train vast parameters. However, it takes significant effort to annotate a large histo-pathology dataset. We introduce a light-weight and interpretable model for nuclei detection and weakly-supervised segmentation. It only requires annotations on isolated nucleus, rather than on all nuclei in the dataset. Besides, it is a generative compositional model that first locates parts of nucleus, then learns the spatial correlation of the parts to further locate the nucleus. This process brings interpretability in its prediction. Empirical results on an in-house dataset show that in detection, the proposed method achieved comparable or better performance than its deep network counterparts, especially when the annotated data is limited. It also outperforms popular weakly-supervised segmentation methods. The proposed method could be an alternative solution for the data-hungry problem of deep learning methods.

Keywords: Nuclei detection and segmentation · Weakly-supervised

1 Introduction

Histopathology images provide an understanding of the microenvironment of various diseases. Nuclei detection and segmentation plays an important role for the analysis of cell morphology and organization. Unfortunately, the non-uniform chromatin texture, irregularity in size and shape as well as touching cells and background clutters put a big challenge to automated nuclei detection and segmentation [2,13,24].

Supplementary Information The online version contains supplementary material available at https://doi.org/10.1007/978-3-031-16961-8_15.

Y. Huo et al. (Eds.): MOVI 2022, LNCS 13578, pp. 145–155, 2022.
https://doi.org/10.1007/978-3-031-16961-8_15

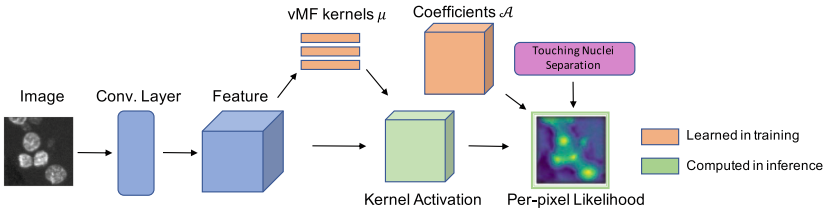

Fig. 1. Flowchart of the proposed method for nuclei detection. A convolution layer is used as feature extractor. For training, we cropped nucleus image patches and learn model parameters (μ and $\mathcal{A}$) in an unsupervised way. In testing, we compute the nucleus existence probability with learned parameters, together with a shape decomposition algorithm to separate touching nuclei, to obtain a per-pixel likelihood prediction.

Recently, deep convolutional neural networks (DNNs) have shown remarkable and reliable performance in histopathology image nuclei detection and segmentation [5,12,16,23,28]. Some works adapt a top-down object detector such as Faster RCNN [18] to histopathology images [3,4]. Others formalize detection as regression to a proximity map, where values on the proximity map represent the proximity to or probability of a nucleus center [8,21,26]. However, the collection of a large number of annotated data is critical and becomes a bottleneck to train conventional DNNs for the analysis of new modalities. To address this issue, there have been interests in nuclei segmentation with weak supervision. Most works in this direction exploited pseudo labels such as progressive model output [14], Voronoi and clustering labels [17], and super-pixel [6]. Nevertheless, a large collection of data is still needed, and most works regard DNNs as a black box without exploring its hidden representations, thus having little interpretability in their decision process. Considering nuclei shapes are invariant to stains, generative models for nuclei detection and segmentation learned from a small dataset are an alternative for efficient and robust analysis of pathology images.

In this study, we propose a light-weight interpretable model for nuclei detection and weakly supervised segmentation. We aim to design a generative model for a single nucleus, therefore only annotations on isolated nucleus are required, which significantly reduces the annotation cost. Inspired by the Compositional Networks [11], we developed a model that do explicit compositional modeling of a nucleus. In this way, the proposed method is able to locate nuclei by finding image regions that it can explain with high probability, and give human interpretable explanations for its prediction. To the best of our knowledge, we are the first to adapt Compositional Networks to nuclei detection and segmentation on histopathology images. To further boost the performance at touching nuclei that are hard to locate and segment precisely, we introduce a non-learning algorithm that requires no annotations to separate touching nuclei. Near-convex shape decomposition has been widely studied in its application to segment binary shapes into parts. However, little has been studied in its effectiveness in separating touch nuclei in histopathology images. We adapted a near-convex shape decomposition algorithm by developing novel ways of defining cuts and assigning

pathologically reasonable weights to the cuts, which proved to be well suited for this task. The output of the separation algorithm is integrated into the compositional model. Empirical results on an in-house DAPI (4',6-diamidino-2-phenylindole) stained pathology image dataset demonstrate the effectiveness and data efficiency of the proposed method for nuclei detection and weakly-supervised segmentation.

2 Method

In Sect. 2.1, we discuss Compositional Network [11], which was originally introduced for natural image classification. We discuss its interpretability for nuclei detection in Sect. 2.2. Section 2.3 discusses our extension based on the Compositional Networks to multiple instance detection, where each nucleus is regarded as an object instance. Finally, in Sect. 2.4, we utilize the prior knowledge about the near-convex shape of nuclei, and introduce near-convex shape decomposition into the developed model, which further facilitates the separation of touching nuclei. The whole flowchart is illustrated in Fig. 1.

2.1 Compositional Networks for Nuclei Modeling

Compositional Network [11] explains the feature map from a convolutional layer in a generative view. Denote a feature map as $F \in \mathbb{R}^{H\times W\times D}$, with H and W being the spatial size and D being the channel size. The feature vector f_i at position i are assumed independently generated, and each is modeled as a mixture of von-Mises-Fisher (vMF) distributions:

$$p(F|\mathcal{A}, \Lambda) = \prod_i p(f_i|\mathcal{A}_i, \Lambda), \tag{1}$$

$$p(f_i|\mathcal{A}_i, \Lambda) = \sum_k \alpha_{i,k} p(f_i|\mu_k), \tag{2}$$

$$p(f_i|\mu_k) \propto \exp\{\sigma f_i^T \mu_k\}, ||f_i|| = 1, ||\mu_k|| = 1, \tag{3}$$

where $\Lambda = \{\mu_k\}$ are kernels for vMF distribution, which can be regarded as the "mean" feature vector of each mixture component k, and $\mathcal{A}_i = \{\alpha_{i,k}\}$ are the spatial coefficients, which learn the probability of μ_k being activated at position i. We say that a vMF kernel μ_k is activated at position i if f_i and μ_k have a high cosine similarity. We set the hyperparameter $\sigma = 30$ for tractability. Given a set of feature maps, the mixture coefficients $\{\alpha_{i,k}\}$ and the vMF kernels $\{\mu_k\}$ can be learned via Maximum Likelihood Estimation in an unsupervised way.

2.2 Interpretable Modeling of Nucleus

An important property of convolutional networks is that the spatial information is preserved in the feature maps. To utilize this property, the set of spatial

coefficients $\{\alpha_{i,k}\}$ are introduced to describe the expected activation of a kernel μ_k at a position i. Thus, α_k at all positions can be intuitively thought of as a 2D template, which depicts the expected spatial activation pattern of parts of a nucleus – *e.g.* where the edges are expected to be located in the image. Therefore, the decision process of the proposed model can be interpreted as first detecting parts, then spatially combining them to get a probability about the nucleus' presence. Note that this implements a part-based voting mechanism.

As the spatial pattern varies dramatically with the shape, size and orientation of nuclei, we further represent F as a mixture of compositional models:

$$p(F|\Theta) = \sum_{m=1}^{M} \nu_m p(F|\mathcal{A}^m), \tag{4}$$

with $\mathcal{V}$=$\{\nu^m \in \{0,1\}, \sum_m \nu_m$=1$\}$. Here M is the number of compositional models in the mixture distribution and ν_m is a binary assignment variable that indicates which compositional model is active. Intuitively, each mixture component m will represent a different set of nuclei with specific shape and size (see Fig. 3 in Appendix). The parameters of the mixture components $\{\mathcal{A}^m\}$ need to be learned in an EM-style manner by iterating between estimating the assignment variables $\mathcal{V}$ and maximum likelihood estimation of $\{\mathcal{A}^m\}$.

2.3 Adaptation to Nucleus Detection

Previous work has proposed to detect salient object in natural images based on Compositional Network [25]. However, it is limited by the assumption that only one salient object is present in an image. Due to the significant difference between histopathology images and natural images, the adaptation for nucleus detection is non-trivial.

First, the background in DAPI stained histopathology images is cleaner than natural images. However, this encourages the model to rely heavily on the background signals, which is undesirable and results in false positives in background regions. We propose to get rid of the disturbance of background signals by masking. For each mixture component m, we pick a subset from $\mathcal{A}^m$ to obtain a soft foreground mask: $M^m = \sum_{k \in K_f} \alpha_k^m$, where K_f is a subset of vMF kernels which represents foreground parts (interior, edge, etc.). Then, we modify the computation of log-likelihood of $p(F|\mathcal{A}^m)$ as:

$$\log p(F|\mathcal{A}^m) = \frac{\sum_i M_i^m \log p(f_i|\mathcal{A}_i^m, \Lambda)}{\sum_i M_i^m} \tag{5}$$

which gives more weights to vMF kernels activated at foreground.

Second, we extend the model to multiple objects by modifying the likelihood:

$$p(\mathcal{F}) = \prod_i \prod_n p(F_i)^{z_{i,n}} \tag{6}$$

where F_i are patches from a whole feature map $\mathcal{F}$, and $\{z_{i,n} \in \{0,1\} | \sum_n z_{i,n} = 1\}$ are indicators of existence of object n at patch F_i. Note that by the design

of the likelihood, only one object model can be active at one position in the feature map. We maximize the likelihood defined in Eq. 6 by applying the model in sliding windows, then selecting the local maxima in the resulted likelihood map after non-maximum suppression.

2.4 Touching Nuclei Separation

Nuclei usually clump and touch with each other, makeing it difficult to recognize single nucleus. The compositional model is able to explain for a single nucleus, but insufficient to separate touching nuclei precisely. We introduce a non-learning algorithm to segment nucleus that requires no annotations. The algorithm is adapted from near-convex shape decomposition [19]. The decomposition output is integrated into the compositional model as a shape prior.

First, we select the vMF kernel μ_0 that respond to the background. Given a feature map F, we compute $1 - \mu_0^T f_i$ at each position i to obtain a nucleus foreground score map. It is further binarized to get foreground connected components. These connected components may consist of a single nucleus or touching nuclei. To distinguish between them, we leverage the following observations: 1) The shapes of nuclei are usually convex. 2) When multiple nuclei cluster together, there are usually concave points along the boundary of the connected component. Based on these observations, we propose to use a near-convex shape decomposition algorithm to process each connected component.

Following [19], a near-convex decomposition of a shape S, $D_\phi(S)$, is defined as a set of non-overlapping parts P_i each with concavity $c(P_i)$:

$$D_\psi(S) = \{P_i | \bigcup_i P_i = S, \forall P_i \cap P_j = \emptyset, c(P_i) \leq \psi\} \tag{7}$$

$$c(P_i) = \max_{v_1, v_2 \in Boundary(P_i)} \{c(v_1, v_2)\} \tag{8}$$

where P_i denotes the decomposed parts; $\psi = 3$ is a parameter for near-convex tolerance. For any two points v_1, v_2 on the boundary of P_i, $c(v_1, v_2)$ is intuitively defined as the max distance from a boundary point u between v_1, v_2 to the line segment $v_1 v_2$. If $c(v_1, v_2) > \psi$, they are named mutex pairs. A set of potential cuts is needed to split S. We compute the curvature of the boundary of S and locate concave points on it. A potential cut is formed by the line segment between two concave points if the line segment lies inside S. To comply with the near-convex constraint, all mutex pairs must be cut into different parts. Furthermore, a specifically designed weight is assigned to each cut, which encourages the selected cuts to be perpendicular to the local boundary and be short, in accord with human intuition. In Appendix 1, we give detailed illustration, formulation and solution for this algorithm.

Nuclei Candidates as Prior. After decomposing the nuclei foreground connected components, the obtained regions are near convex and are taken as candidates of single nucleus. These candidates serve as a prior guiding where to pay attention to for nucleus detection. We define the prior probability of nucleus existence q as Gaussian distributions centered at each candidate. The final detection

probability is obtained by integrating the prior into the compositional model and the final probability map is defined as:

$$p(\mathcal{F}) = \prod_i \prod_n p(F_i)^{z_{i,n}} q(i). \tag{9}$$

2.5 Weakly-Supervised Nuclei Segmentation

The nuclei candidates obtained from Sect. 2.4 can also be used as segmentation masks. Since the algorithm only receives bounding box as supervision which is used to crop nucleus images, it achieves segmentation masks in a weakly-supervised way. The obtained segmentation masks have a property to be near convex. Although rare nuclei can have concave shapes and be wrongly cut, it can be indicative of potential annotation errors (*e.g.* where the annotator mistakenly recognized a pair of touching nuclei as a single one).

3 Experiments and Results

Dataset. Multiplexed immunofluorescence (mIF) and immunohistochemistry (IHC) are emerging technologies with better predictions for immunotherapy [15]. The mIF images were obtained using Vectra-3 and Vectra Polaris microscopes (Akoya BioSciences, MA, USA) from six patients with liver cancer (3), lung adenocarcinoma (1), lung small cell carcinoma (1), and melanoma (1). For the nuclei detection and segmentation, DAPI(4',6-diamidino-2-phenylindole) stained images were used in this study among the multispectral images. The selected images were manually annotated and checked by trained researchers. Totally 18312 nuclei were annotated on 210 images, 186 for training and 24 for testing.

3.1 Nuclei Detection

Baselines & Evaluation Metrics. Our motivation is to develop data-efficient models to save annotation efforts, meanwhile being interpretable. Therefore, we compare our model with a classic baseline patch-CNN [22], and one of the state-of-the-art methods [27], which utilized structured regression with a U-Net-like backbone [20]. For patch-CNN, the model complexity is close to ours and the same patch size was used, which makes the comparison fair. The structured regression (SR) [27] method is trained with full image supervision rather than on isolated nuclei, as it was designed. Therefore, it serves as an upper-bound for comparison. Following [1,7,10,21], we adopt the commonly used precision (P) - recall (R) metrics to evaluate nucleus detection methods.

Implementation Details. The proposed method uses the first layer of a U-Net [20] as a feature extractor, which is pretrained on unsupervised nuclei super-pixel segmentation. It is followed by the generative compositional model defined in Sect. 2. We used 3097 isolated nuclei to learn the model parameters. We empirically found that 12 vMF kernels are sufficient to model different parts of a nucleus (See Fig. 2 in Appendix). The number of compositional models in the

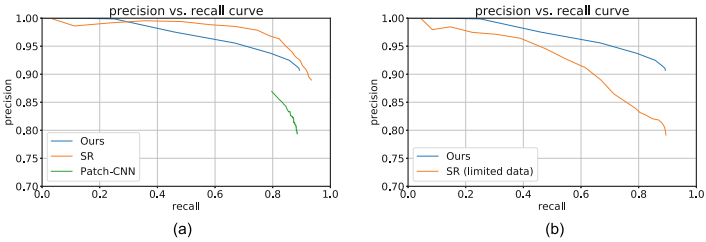

Fig. 2. Evaluation of nucleus detection by Precision-Recall curve. (a) Trained with full data; (b) Trained with 10% data.

mixture is set to $M = 20$, each represents nuclei with a specific size and shape (See Fig. 3 in Appendix). To detect nuclei with various orientations, we rotated input images by every 30°. The hyper-parameters were chosen via evaluation on a validation set.

Results. Figure 2 shows the P-R curve of the baseline Patch-CNN, SR and the proposed method. The proposed method surpasses patch-CNN by a large margin, which shows the effectiveness of the proposed method. We believe this is due to the explicit generative modeling of nuclei features, which boosts performance while keeping the model to be light-weight. Due to extended model complexity and full image supervision training, SR outperforms the proposed method. This is understandable since the SR model is a much deeper network and has a larger field of view with full image supervision. However, deep neural networks like SR are data hungry and require large amounts of data to learn their parameters, while the proposed method only requires the annotations of isolated nuclei, which saves much effort for human experts.

To verify the hypothesis that our method is more data-efficient than deep neural networks, we made a comparison between SR and our method under approximately the same amount of training data in terms of the number of nuclei used. For SR, this was implemented by limiting the number of training images to ensure the total number of nucleus seen in training are about the same. In Fig. 2(b), we can see that when trained with approximately the same amount of data, the performance of SR degrades significantly. This result proves that when large amounts of annotated nuclei samples are not available, our method is able to present superior nuclei detection results than an over-parameterized (in terms of the dataset size) deep neural network.

Table 1. Weakly supervised segmentation performance measured in AJI and DSC on the in-house dataset.

	AJI	DSC
BBTP	0.6765	0.8513
PointAnno	0.5991	0.7805
Ours	**0.7030**	**0.8900**

3.2 Weakly-Supervised Nuclei Segmentation

As stated in Sect. 2.5, by utilizing the unsupervisedly learned vMF kernels and the near-convex decomposition algorithm, we can obtain nuclei instance segmentation masks. We compare with two weakly-supervised segmentation methods, BBTP [9] and PointAnno [17]. BBTP is a well-known weakly-supervised model for natural images, and PointAnno is developed for nuclei segmentation. Aggregated Jaccard Index (AJI) [12] and Dice similarity coefficient (DSC) were used as metrics. AJI focuses more on the correct matching between segmented nuclei instances and ground-truths, while DSC focuses on the foreground/background classification.

Table 1 shows the segmentation performance of the three methods. Our method outperforms BBTP and PointAnno on both AJI and DSC. What's more, our method requires little training (only the clustering of vMF kernels), which is an advantage over deep networks. Qualitative results are shown in Fig. 3. Our method is able to precisely locate the foreground and cut touching nuclei, even for hard cases where more than two nuclei are touching with each other. Compared with BBTP and PointAnno, the segmentation masks obtained by the proposed method aligns better with the ground-truth nuclei contours, thanks to the accurate detection of foreground as well as the cutting at reasonable positions between touching nuclei.

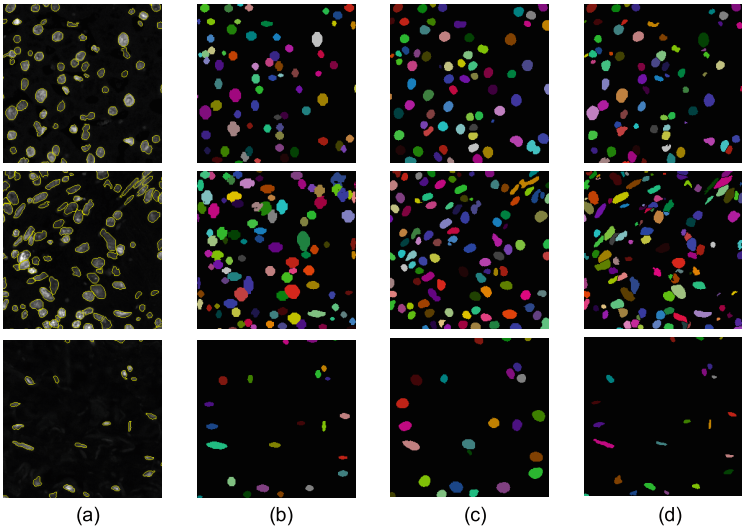

Fig. 3. Qualitative segmentation results. Each line shows one image from the test set and the segmentation masks obtained by three methods on it. (a) is the DAPI stained image with the boundaries of each nucleus annotated. (b) are the predictions of BBTP, (c) are the predictions of PointAnno, and (d) are the predictions of our method.

4 Conclusion

We introduce a light-weight interpretable model for nuclei detection and segmentation. It is data-efficient that ease the data annotation cost for data hungry deep learning methods. In addition, it is interpretable in that it exploits the hidden features and builds probabilistic models for nucleus. We hope our work would contribute to the study of data efficiency and interpretability in the histology image analysis community.

References

1. Alom, M.Z., Yakopcic, C., Taha, T.M., Asari, V.K.: Microscopic nuclei classification, segmentation and detection with improved Deep Convolutional Neural Network (DCNN) approaches (2018)
2. Arteta, C., Lempitsky, V., Noble, J.A., Zisserman, A.: Learning to detect cells using non-overlapping extremal regions. In: Ayache, N., Delingette, H., Golland, P., Mori, K. (eds.) MICCAI 2012. LNCS, vol. 7510, pp. 348–356. Springer, Heidelberg (2012). https://doi.org/10.1007/978-3-642-33415-3_43
3. Baykal, E., Dogan, H., Ercin, M.E., Ersoz, S., Ekinci, M.: Modern convolutional object detectors for nuclei detection on pleural effusion cytology images. Multimed. Tools App. **79**(21-22), 15417–15436 (2020). https://doi.org/10.1007/s11042-019-7461-3
4. Du, J., Li, X., Li, Q.: Detection and classification of cervical exfoliated cells based on faster R-CNN. In: 2019 IEEE 11th International Conference on Advanced Infocomm Technology, ICAIT 2019 (2019). https://doi.org/10.1109/ICAIT.2019.8935931
5. Graham, S., et al.: Hover-Net: simultaneous segmentation and classification of nuclei in multi-tissue histology images. Med. Image Anal. **58**, 101563 (2019)
6. Guo, R., Pagnucco, M., Song, Y.: Learning with noise: mask-guided attention model for weakly supervised nuclei segmentation. In: de Bruijne, M., et al. (eds.) MICCAI 2021. LNCS, vol. 12902, pp. 461–470. Springer, Cham (2021). https://doi.org/10.1007/978-3-030-87196-3_43
7. Hagos, Y.B., Narayanan, P.L., Akarca, A.U., Marafioti, T., Yuan, Y.: ConCORDe-Net: cell count regularized convolutional neural network for cell detection in multiplex immunohistochemistry images. In: Shen, D., et al. (eds.) MICCAI 2019. LNCS, vol. 11764, pp. 667–675. Springer, Cham (2019). https://doi.org/10.1007/978-3-030-32239-7_74
8. Höfener, H., Homeyer, A., Weiss, N., Molin, J., Lundström, C.F., Hahn, H.K.: Deep learning nuclei detection: a simple approach can deliver state-of-the-art results. Computerized Medical Imaging and Graphics **70**, 43–52 (2018). https://www.sciencedirect.com/science/article/pii/S0895611118300806
9. Hsu, C.C., Hsu, K.J., Tsai, C.C., Lin, Y.Y., Chuang, Y.Y.: Weakly supervised instance segmentation using the bounding box tightness prior. In: Advances in Neural Information Processing Systems, vol. 32 (2019)
10. Kashif, M.N., Raza, S.E., Sirinukunwattana, K., Arif, M., Rajpoot, N.: Handcrafted features with convolutional neural networks for detection of tumor cells in histology images. In: Proceedings - International Symposium on Biomedical Imaging. vol. 2016-June (2016)

11. Kortylewski, A., Liu, Q., Wang, A., Sun, Y., Yuille, A.: Compositional convolutional neural networks: a robust and interpretable model for object recognition under occlusion. Int. J. Comput. Vis. **129**(3), 736–760 (2021)
12. Kumar, N., Verma, R., Sharma, S., Bhargava, S., Vahadane, A., Sethi, A.: A dataset and a technique for generalized nuclear segmentation for computational pathology. IEEE Trans. Med. Imaging **36**(7), 1550–1560 (2017)
13. Kuse, M., Wang, Y.F., Kalasannavar, V., Khan, M., Rajpoot, N.: Local isotropic phase symmetry measure for detection of beta cells and lymphocytes. J. Pathol. Inform. **2**, 2 (2011)
14. Lee, H., Jeong, W.-K.: Scribble2Label: scribble-supervised cell segmentation via self-generating pseudo-labels with consistency. In: Martel, A.L., et al. (eds.) MICCAI 2020. LNCS, vol. 12261, pp. 14–23. Springer, Cham (2020). https://doi.org/10.1007/978-3-030-59710-8_2
15. Lu, S., et al.: Comparison of biomarker modalities for predicting response to PD-1/PD-L1 checkpoint blockade: a systematic review and meta-analysis. JAMA Oncol. **5**(8), 1195–1204 (2019)
16. Naylor, P., Lae, M., Reyal, F., Walter, T.: Nuclei segmentation in histopathology images using deep neural networks. In: Proceedings - International Symposium on Biomedical Imaging (2017)
17. Qu, H., et al.: Weakly supervised deep nuclei segmentation using partial points annotation in histopathology images. IEEE Trans. Med. Imaging **39**(11), 3655–3666 (2020)
18. Ren, S., He, K., Girshick, R., Sun, J.: Faster R-CNN: towards real-time object detection with region proposal networks. In: Advances in Neural Information Processing Systems, vol. 28 (2015)
19. Ren, Z., Yuan, J., Li, C., Liu, W.: Minimum near-convex decomposition for robust shape representation. In: Proceedings of the IEEE International Conference on Computer Vision (2011)
20. Ronneberger, O., Fischer, P., Brox, T.: U-net: convolutional networks for biomedical image segmentation. In: Navab, N., Hornegger, J., Wells, W.M., Frangi, A.F. (eds.) MICCAI 2015. LNCS, vol. 9351, pp. 234–241. Springer, Cham (2015). https://doi.org/10.1007/978-3-319-24574-4_28
21. Sirinukunwattana, K., Ahmed Raza, S.E., Tsang, Y.-W., Snead, D., Cree, I., Rajpoot, N.: A spatially constrained deep learning framework for detection of epithelial tumor nuclei in cancer histology images. In: Wu, G., Coupé, P., Zhan, Y., Munsell, B., Rueckert, D. (eds.) Patch-MI 2015. LNCS, vol. 9467, pp. 154–162. Springer, Cham (2015). https://doi.org/10.1007/978-3-319-28194-0_19
22. Sirinukunwattana, K., Raza, S.E., Tsang, Y.W., Snead, D.R., Cree, I.A., Rajpoot, N.M.: Locality sensitive deep learning for detection and classification of nuclei in routine colon cancer histology images. IEEE Trans. Med. Imaging **35**(5), 1196–1206 (2016)
23. Tofighi, M., Guo, T., Vanamala, J.K., Monga, V.: Deep networks with shape priors for nucleus detection. In: Proceedings - International Conference on Image Processing, ICIP (2018)
24. Veta, M., Van Diest, P.J., Kornegoor, R., Huisman, A., Viergever, M.A., Pluim, J.P.: Automatic nuclei segmentation in h&e stained breast cancer histopathology images. PloS ONE **8**(7), e70221 (2013)
25. Wang, A., Sun, Y., Kortylewski, A., Yuille, A.: Robust object detection under occlusion with context-aware compositionalNets. In: Proceedings of the IEEE Computer Society Conference on Computer Vision and Pattern Recognition (2020)

26. Xie, Y., Xing, F., Kong, X., Su, H., Yang, L.: Beyond classification: structured regression for robust cell detection using convolutional neural network. In: Navab, N., Hornegger, J., Wells, W.M., Frangi, A.F. (eds.) MICCAI 2015. LNCS, vol. 9351, pp. 358–365. Springer, Cham (2015). https://doi.org/10.1007/978-3-319-24574-4_43
27. Xie, Y., Xing, F., Shi, X., Kong, X., Su, H., Yang, L.: Efficient and robust cell detection: a structured regression approach. Med. Image Anal. **44**, 245–254 (2018)
28. Xu, J., Xiang, L., Liu, Q., Gilmore, H., Wu, J., Tang, J., Madabhushi, A.: Stacked sparse autoencoder (SSAE) for nuclei detection on breast cancer histopathology images. IEEE Trans. Med. Imaging **35**(1), 119–130 (2016)